Journal Name, under review, pp. 1–15

doi: DOI HERE
Advance Access Publication Date: Day Month Year
Original Article

ORIGINAL ARTICLE

The subcortical basis of subjective sleep quality

Martin M. Monti[1,2*]

[1]Department of Psychology, University of California Los Angeles, 502 Portola Plaza, Los Angeles, 90095, CA, USA and [2]Brain Injury Research Center (BIRC), Department of Neurosurgery, University of California Los Angeles, 300 Stein Plaza Driveway, Los Angeles, 90095, CA, USA
*Corresponding author: monti@ucla.edu
FOR PUBLISHER ONLY Received on Date Month Year; revised on Date Month Year; accepted on Date Month Year

Abstract

Study objectives: To assess the association between self-reported sleep quality and cortical and subcortical local morphometry.
Methods: Sleep and neuroanatomical data from the full release of the young adult Human Connectome Project dataset were analyzed. Sleep quality was operationalized with the Pittsburgh Sleep Quality Index (PSQI). Local cortical and subcortical morphometry was measured with subject-specific segmentations resulting in voxelwise thickness measurements for cortex and relative (i.e., cross-sectional) local atrophy measurements for subcortical regions.
Results: Relative atrophy across several subcortical regions, including bilateral pallidum, striatum, and thalamus, was negatively associated with both global PSQI score and sub-components of the index related to sleep duration, efficiency, and quality. Conversely, we found no association between cortical morphometric measurements and self-reported sleep quality.
Conclusions: This work shows that subcortical regions such as the bilateral pallidum, thalamus, and striatum, might be interventional targets to ameliorate self-reported sleep quality.

Key words: Sleep, Sleep Quality, Anatomy, Thalamus, Globus Pallidus, Striatum

Introduction

Highly conserved across the animal kingdom [1], sleep is important for cognitive, social, and emotional functioning [2–4] across the lifespan [5, 6]. Indeed, sleep deprivation has been associated with cognitive and emotional dysfunction [7–12], sleep disturbances are associated with psychiatric illnesses [13–16] and are part of the known non-motor symptomatology of multiple neurodegenerative disorders [17–22].

Despite the importance of sleep, our understanding of its relationship with brain morphology remains in the early phases [23, 24]. Furthermore, while large-sample studies are now starting to emerge [25–29], the results are yet to coalesce and remain variable, perhaps also due to different methodological choices [30], often with relatively small effect sizes despite increasingly sophisticated approaches. Yet, a greater understanding of the relationship between brain structures and sleep is key to devising new interventions to mitigate sleep-related disorders [31].

In what follows, we leverage the full release of the Human Connectome Project (HCP) [32], to assess the relationship between subjective sleep quality indicators [33] and brain morphometry using local (i.e., voxelwise) cortical [34, 35] and subcortical [36] morphometry, as opposed to the global and regional features (i.e., average regional volumes, areas, and thickness) used in prior work [26, 28, 29]. Specifically, we show that the global PSQI score, and subcomponents associated with sleep duration, efficiency, and quality, are inversely associated with widespread subcortical local atrophy.

Methods

Sample description

This project is based on the Q3 release of the Human Connectome Project (HCP; [32]). Out of the 1206 total participants, 93 could not be included in the analysis due to failure to acquire at least one T1-weighted MRI dataset, resulting in an included sample of 1,113 datasets. (As described below, one additional dataset was excluded due segmentation failure, resulting in a final analyzed sample of 1,112 datasets). The final analyzed sample included data from 605 female and 507 male, with 231 individuals in the 22-25 age group, 486 in the 26-30 age group, 382 in the 31-35 age group, and 13 individuals 36 years old or greater.

PSQI data

For each participant, we collected the total score and the individual component scores of the Pittsburgh sleep Quality Index (PSQI; [33]) as made available in the most recent HCP data distribution. Because of extensive correlations across the seven components of the PSQI (see SOM1), prior to analyzing their relationship to brain structures, we performed a data reduction use a Principal Component Analysis (PCA; [37]) approach. The PCA was performed in JASP 2024 (v 0.18.3;

© The Author *under review*.

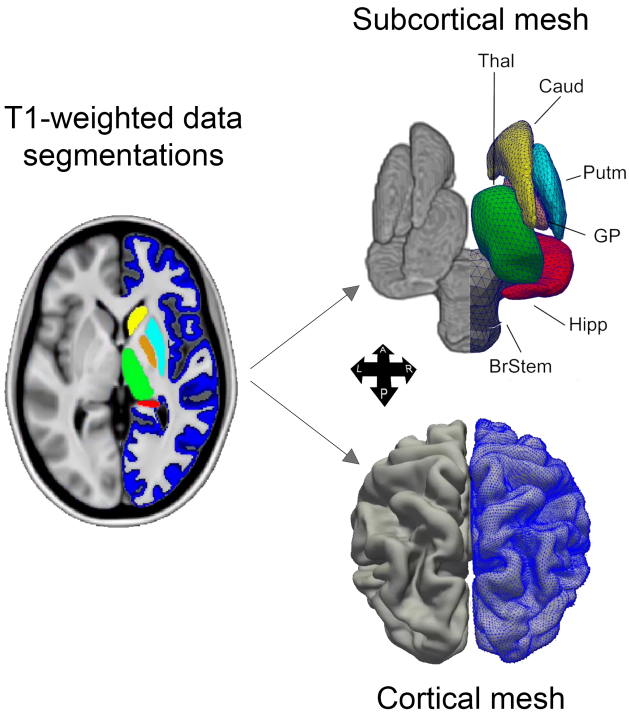

Fig. 1. Methods. Left: Illustration of cortical and subcortical segmentations of the T1-weighted data. Right: Illustration of 3D subcortical (top) and cortical (bottom) reconstructed meshes. (Image partially adapted from [39])

[38]), using an orthogonal varimax rotation and retaining all components with an eigenvalue greater than 1. This data reduction resulted in two orthogonal components explaining 50% of the variance. As shown in Tab. 1, the first principal component loaded mainly on the sleep quality, sleep duration, and sleep efficiency PSQI components (with loadings equal to 0.62, 0.83, and 0.74, respectively). The second principal component loaded mainly on the sleep onset latency, sleep disturbances, and use of sleep medications PSQI components (with loadings equal to 0.67, 0.61, and 0.69, respectively). The daytime dysfunction PSQI component was loaded upon very weakly (< 0.36) by both PCs.

MRI data

A total of 1,113 T1-weighted data were obtained from the HCP Young Adult repository. For this project we selected, for each participant, the "T1w_MPR1" dataset acquired as part of the "structural session". As described in the HCP Q3 release appendix (available at http://www.humanconnectome.org) these data were acquired with a Magnetization-Prepared Rapid Acquisition Gradient Echo (MPRAGE) sequence (TR = 2,400 ms, TE = 2.14 ms, TI = 1,000 ms, GRAPPA acceleration factor = 2). The acquisition resulted in an image size of $256 \times 320 \times 243$ voxels (in the x, y, and z directions, respectively) and an isovoxel resolution of 0.7 mm.

MRI data analysis

T1-weighted data preprocessing and segmentation

All MRI data analyses were performed with the FMRIB Software Library (FSL; [40]). T1-weighted data were first preprocessed using the `fsl_anat` script, which provides a general pipeline for processing anatomical images. For each dataset, the script reorients images to the standard (MNI) orientation (`fslreorient2std`), crops the image (`robustfov`), performs bias-field correction (RF/B1-inhomogeneity-correction; `FAST`; [41]), registration to standard space (linear and non-linear; `FLIRT` and `FNIRT`, [42, 43]), brain-extraction (`FNIRT`-based), tissue-type segmentation (`FAST`; [41]), and subcortical structure segmentation (`FIRST`; [36]). Once subcortical segmentations were completed, and before any analysis, the resulting subcortical meshes were individually inspected by the author to ensure correct structure segmentation (cf., Fig. 1). During this control, it emerged that segmentation for one dataset failed, not producing any mesh output. That dataset was thus excluded from any further analysis (leading to a final analyzed sample of 1,112 datasets). Cortical segmentations were obtained by feeding the bias-corrected T1-weighted data to FSL Voxel Based Morphometry (VBM; [44]) scripts, an optimized VBM protocol [35] enclosed in the FSL distribution. Again, segmentations were visually inspected for accuracy prior to any analysis. All 1,112 datasets return satisfactory segmentations of the cortical gray matter (cf., Fig. 1).

T1-weighted data analysis

The obtained single subject cortical segmentations and subcortical meshes were entered into a group VBM analysis and a group shape (or vertex) analysis, respectively. While both cortical and subcortical tissues are segmented in the subject's native space, subcortical meshes are then co-registered to the standard MNI space for the purposes of group analysis. Conversely, cortical segmentations are co-registered to an *ad-hoc* sample-specific template created, automatically, as an average of all the $1,112$ input data, for the purposes of performing the VBM group analysis. Each set of segmentations (i.e., cortical, subcortical) were entered into two group analyses. First, we regressed the segmentations on the PSQI total score (henceforth, PSQI total score analysis). Second, we regressed the segmentations the two PCA components described above (henceforth, PSQI PCA analysis). In addition to these regressors of interest, each of these two statistical models also included sex and age-group covariates, as well as each subject's total normalized brain volume (as calculated with SIENAX; [45]) in order to account for the effect of head size variability across individuals and to ensure that results reflect local shape change [39, 46].

Group analyses were performed with Randomise [47] using a non-parametric permutation testing approach [48]. Significance was assessed against a criterion of $\alpha \leq 0.05$ corrected for multiplicity with a family-wise cluster correction approach with 2-dimensional Threshold Free Cluster Enhancement (TFCE; [49, 50]).

Results

PSQI data analysis

As shown in Fig. 2 and in Tab. 1, the PSQI total score in the analyzed sample had a mean of 4.8 and a median of 4. Using the conventional criterion of PSQI 5 [33], 38% of participants in the analyzed sample were classified as having poor sleep quality. The proportion of poor sleepers was not significantly different across male and female participants (i.e., 31% and 33% for male and female, respectively; $\chi^2(1) = 0.685$, p= 0.408) nor across

the four age groups (i.e., 33%, 33%, 31%, and 21% for the 22-25, 26-30, 31-35, and over 35 age groups, respectively; $\chi^2(3) = 0.932$, p= 0.818).

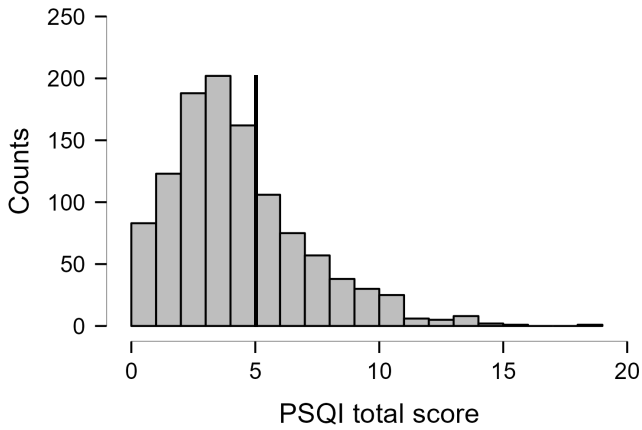

Fig. 2. Distribution of PSQI total scores in the analyzed sample. The black line indicates the conventional criterion discriminating "bad sleepers" (i.e., PSQI total score > 5) from "good sleepers" (i.e., PSQI total score ≤ 5; [33]).

Table 1. Characteristics of the PSQI total score and each component, for the analyzed sample. (Abbreviations: Std. Dev., standard deviation; Min., minimum; Max., maximum; PC, principal component; Tot., total; sleep qual., sleep quality; sleep ons. lat., sleep onset latency; sleep dur., sleep duration; sleep effic., sleep efficiency; sleep disturb., sleep disturbances; use of sleep med., use of sleep medications; daytime dysf., daytime dysfunction.)

PSQI	Mean	Std. Dev.	Min.	Max.	PC
Tot. Score	4.80	2.76	0	19	
PSQI comp.					
Subj. sleep qual.	0.89	0.63	0	3	1
Sleep ons. lat.	0.97	0.82	0	3	2
Sleep dur.	0.57	0.82	0	3	1
Sleep effic.	0.46	0.79	0	3	1
Sleep distrub.	1.09	0.49	0	3	2
Use of sleep med.	0.24	0.68	0	3	2
Daytime dysf.	0.59	0.64	0	3	-

MRI results

As shown in Fig. 3 and Tab. 2 (see also SOM2), the PSQI total score analysis resulted in extensive negative correlations with many subcortical regions. Specifically, extensive negative associations were found between the PSQI total score and atrophy in the bilateral pallidum (99.2% and 97.6% of left and right hemisphere voxels, respectively), thalamus (96.1% and 99.3% of left and right hemisphere voxels, respectively), putamen (91.3% and 89.1% of left and right hemisphere voxels, respectively), and caudate (64.7% and 83.0% of left and right hemisphere voxels, respectively). Additionally, regions of significant negative association with the PSQI total score were also observed in the left nucleus accumbens and amygdala (64.7% and 45.8% of voxels, respectively), bilateral hippocampus (27.1% and 6.7% of left and right hemisphere voxels, respectively), and in the brainstem (20.2% of voxels). No positive correlations were detected between PSQI total score and subcortical shape. Similarly, no associations were found, either positive or negative, with cortical thickness.

The PSQI PCA analyses returned significant negative associations between PC1 and most of the regions found in the PSQI total score analysis regions (cf., Fig. 3 and Tab. 2). Specifically, significant negative associations were observed in the bilateral pallidum (91.1% and 89.8% of left and right hemisphere voxels, respectively), putamen (86.0% and 82.3% of left and right hemisphere voxels, respectively), caudate (66.9% and 82.3% of left and right voxels, respectively), and thalamus (67.6% and 82.3% of left and right hemisphere voxels, respectively). Smaller areas of significant negative association with PC1 were also uncovered in the left nucleus accumbens (35.6% of voxels) and amygdala (32.3% of voxels), and right hippocampus (1.6% of voxels). No positive associations were found between PC1 and subcortical local morphometry. Similarly, no associations were found, either positive or negative, between subcortical local morphometry and PC2. Mirroring the first analysis, no associations were found, either positive or negative, between local cortical measurements and either PC.

Given the null voxelwise cortical results, in order to assess whether this was due to the specific analytical protocol employed [51], we leveraged the existing global, cortical and subcortical morphometric analyses made available as part of the HCP data distribution (and comparable to some of the measurements discussed in prior work [28, 29]). As described elsewhere [52], this volumetric analysis is based on a different software than the analysis reported above (i.e., FreeSurfer version 5.2 [53, 54], as opposed to FSL) and a different processing pipeline (i.e., the so-called HCP minimal processing structural pipeline [52], obtained by running three scripts included in FreeSurfer : *PreFreeSurfer*, *FreeSurfer*, and *PostFreeSurfer*). When we performed a Mann-Whitney independent samples test (due to violation of normality, as assessed with a Shapiro-Wilk test [55]) comparing "good sleepers" versus "bad sleepers," only two out of the 199 global and region-specific morphometric measurements available exhibited a significant difference between the two groups (using the Benjamini Hochberg FDR adjustment for multiplicity [56]): cortical thickness in the right entorhinal and temporal pole cortices (cf., Table SOM1). Beyond that, we found no association between any of the remaining global and local (including regional thickness, area, and volume) measurement and self-reported sleep quality (cf., Table SOM1).

Discussion

In the present work, we report two main results. First, we show that sleep quality, as assessed by the PSQI total score, as well as by specific PSQI components (i.e., quality, duration, and efficiency; cf., 1), are associated with significant inwards displacement of several subcortical areas including, in particular, the bilateral globus pallidus, thalamus, and the striatum. Conventionally, this result is interpreted as indicating that worse sleep quality is associated with local atrophy (cross-sectionally) in these regions [36]. Associations between subcortical regions and sleep have a long history in the context of pre-clinical animal models [57, 58]. Only more recently this association has returned to the forefront [31, 59, 60]. In particular, our results show maximal association

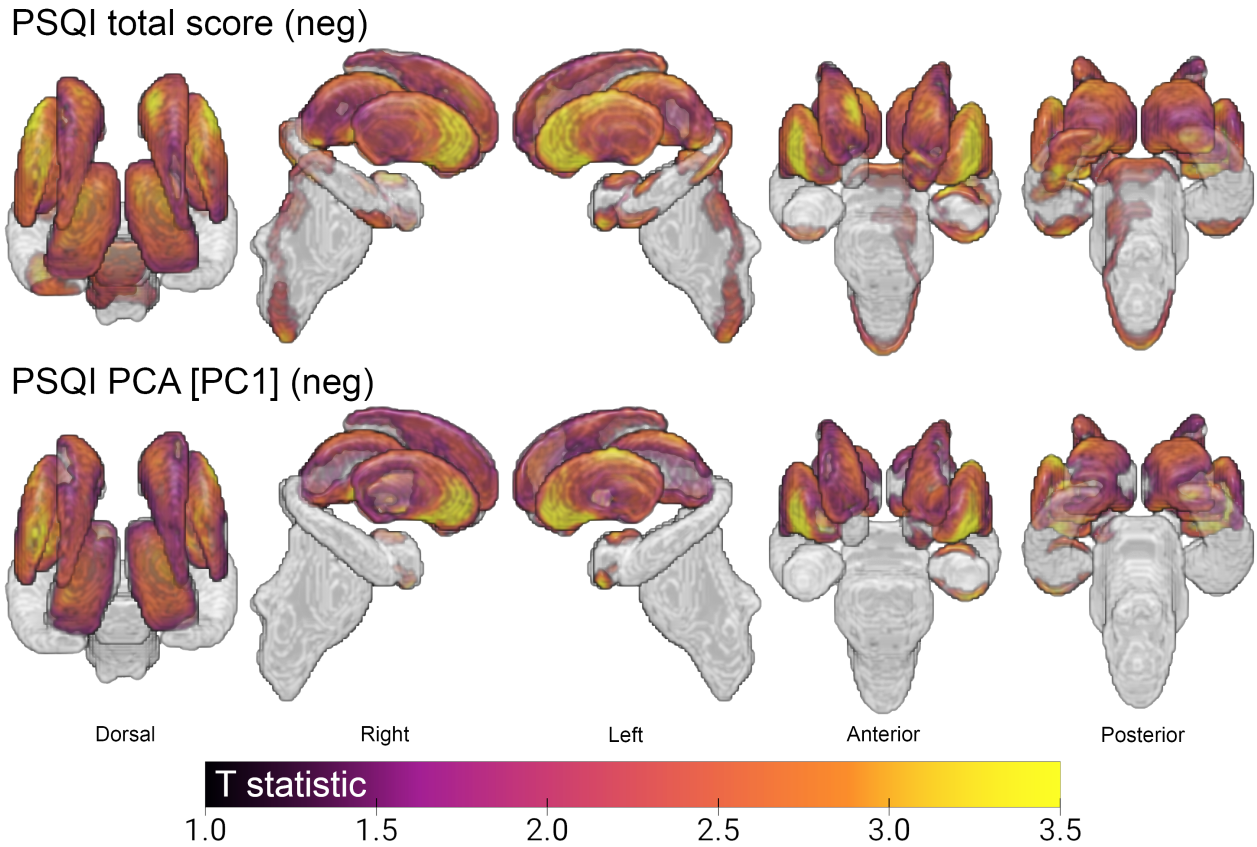

Fig. 3. Subcortical results. Areas significantly associated, negatively, with the PSQI total score analysis (top) and the PSQI PCA analysis (PC1). (Areas shown in color indicate significant voxels. Areas shown in gray imply no significant result.)

between the PSQI measures (total, as well as PC1) and bilateral globus pallidus (cf., Fig. SOM), striatum, and thalamus.

Thalamus, and its interactions with cortex, have long been implicated in sleep-wake transitions, as a key target of ascending arousal system [61, 62]. Indeed, sleep disturbances are associated with thalamic abnormalities and/or dysfunction across a large set of mental health and neuropsychiatric disorders. In patients with insomnia, for example, clinical features of the pathology are associated with thalamic structural and functional abnormalities [63, 64]. Aberrant metabolite levels in thalamus have been found, in multiple diseases, to be associated negatively with sleep quality measurements [65, 66]. Furthermore, long-term sleep deprivation is known to be associated with decreased thalamic volume [67], while thalamic stroke and infarction are known to lead to sleep impairments [68, 69]. Even in healthy volunteers, across the lifespan, thalamic volumes and function are associated with sleep disturbances [70].

Long known to serve a key role in the control of motor behavior [71], the contributions of the basal ganglia to non-motor function have only come to the forefront relatively recently [59, 60], together with a renewed understanding of the complex circuitry tying these regions together and within broader cortical-subcortical circuits [31, 72, 73]. Indeed, clinical data show that patients with striatal dysfunction syndromes, such as Parkinson's and Huntington Disease, exhibit high rates of sleep disturbances [17–20, 74], something that is likely to be mediated, at least in part, by dopamine mechanisms [75]. Interestingly, the availability of striatal dopamine in D2/D3 receptors has been associated with sleep quality in healthy adults [76]. Consistent with this view, and with our findings in healthy volunteers, lesion studies in the rodent model have documented alteration of sleep-wake behavior following striatal damage [58, 77]. In particular, striatal lesions have been shown to lead to an increased number of state transitions and loss of ultra-long wake bouts (i.e., greater sleep fragmentation) [78]. In addition, the role of dopamine in modulating sleep-wake behavior might rely on the action of a number of subcortical regions, including the nucleus accumbens [78–80], a regions which we also find to be atrophic in individuals with poorer sleep quality. It is not surprising, then, that despite a certain heterogeneity in findings, self-reported sleep has been associated multiple time to neuroanatomical measurements in these regions [28, 29].

The region most extensively associated with our measures of sleep quality (i.e., PSQI total score and PSQI PC1) was the bilateral globus pallidus. Traditionally conceived as a relay in the control of motor behavior [81–83], a growing amount of evidence is linking this region – and its external portion in particular – to the regulation of sleep-wake behavior and electrophysiology [59, 60], likely *via* dopaminergic neuromodulation [84]. Indeed, as found with the striatum, excitotoxic lesions of the external portion of the pallidum, in rodent models, increase sleep fragmentation, with increased sleep-wake transitions and decreased sleep bouts [78, 85]. Conversely, optogenetic and electical neuromodulation of this

Table 2. Subcortical results. Proportion of significant voxel for each subcortical structure. (Abbreviations: Hem., hemisphere; Prop. Sig. Voxels, Proportion of Significant Voxels; L, left; R, Right)

Structure	Hem.	Prop. Sig. Voxels (%)
PSQI total score analysis (negative association)		
Thalamus	R	99.27%
Pallidum	L	99.19%
Pallidum	R	97.62%
Thalamus	L	96.10%
Putamen	L	91.32%
Putamen	R	89.07%
Caudate	R	83.04%
Nucleus Accumbens	L	64.71%
Caudate	L	64.08%
Amygdala	L	45.77%
Hippocampus	L	27.06%
Brain Stem		20.21%
Hippocampus	R	6.67%
Nucleus Accumbens	R	0.00%
Amygdala	R	0.00%
PSQI PCA analysis		
PC1 (neg. association)		
Pallidum	L	91.05%
Pallidum	R	89.77%
Putamen	L	86.03%
Caudate	R	82.34%
Thalamus	R	82.28%
Putamen	R	75.82%
Thalamus	L	67.61%
Caudate	L	66.91%
Nucleus Accumbens	L	35.85%
Amygdala	L	32.36%
Hippocampus	R	1.57%
Brain Stem		0.00%
Hippocampus	L	0.00%
Nucleus Accumbens	R	0.00%
Amygdala	R	0.00%

region results in a broad increase of time spent sleeping [85, 86]. Consistent with these findings, in humans, the pallidum has been associated to behavioral and/or electrocortical arousal in healthy volunteers undergoing general anesthesia [87], and in severe brain injury patients [39, 46]. Intriguingly, and mirroring the rodent work, deep brain stimulation of the external portion of the pallidum in a parkinsoninan patient dramatically improved their sleep [88].

Finally, although to a much smaller extent than the regions discussed above, we also found systematic associations between worse subjective sleep quality and amygdalar and hippocampal atrophy. With respect to the latter, prior work suggests a negative relation between hippocampal morphometry and self-reported sleep indices both cross-sectionally [29] and longitudinally [26]. Furthermore, we highlight that, considering the relatively small effect sizes reported in prior work, the fact that we uncover a similar association, in a small portion of the hippocampus, in a different sample, and with a different methodology, offers concordant evidence for hippocampus playing a role in explaining individual differences in self-reported sleep. With respect to the amygdala, our findings are consistent with prior reports associating amygdalar atrophy, connectivity dysfunction, and sleep disturbances across a number of conditions [29, 89–92], dissociably from its comorbid association with anxiety [93].

Our second main finding is that, in stark contrast to the subcortical results, we find no association between voxelwise cortical thinning and self-reported measures of sleep quality. This general result agrees with a recent very large sample report [28], but stands in contrast with prior some studies reporting associations between cortical morphometric measurements and sleep [29, 94]. Interestingly, even when we assessed regional (and global) morphometric measurements similarly to prior studies [29, 94], we find only 2 significant associations with sleep quality, with overwhelmingly small effect sizes (cf., Tab. SOM1), with only one of the two (in the hippomampal complex) matching prior reports, despite using comparable analytical methods [30]. It remains to be resolved in future work whether the variance in cortical results is genuine or reflects, to some extent, the known greater variability in cortical, versus subcortical, neuroanatomy [95].

In assessing the present findings, one must take stock of a number of limitations tied to the analytical approach employed. First, the segmentation technique we used [36] cannot capture a number of important regions and subregions that are believed to play an important role in the regulation of sleep-wake behavior [96, 97]. Second, our morphometric approach is unable to capture non-neural systems which have been proposed to play an important role in sleep (e.g., the glymphatic system) [98]. Finally, this work is focused entirely on neuroanatomical variability, yet there exist known associations between changes in brain function and sleep quality [99–102]. It will be interesting, in future work, to delineate the degree to which (if any) the known associations between brain network function and perceived sleep quality [103, 104] is related to the neuroanatomical variability described in the present work.

Conclusion

Overall, the present work shows that subjective sleep quality, as captured by conventional self-report [33], in the general population is directly related to the shape of subcortical nodes and, in particular, the globus pallidus, striatum, and thalamus. Importantly, we show that it is not necessarily the overall volume of these regions that is associated with sleep quality, but rather the specific topological focus of thinning/atrophy. This work shows that subcortical regions, including the globus pallidus, thalamus, and the striatum, might be potential targets to ameliorate sleep in otherwise healthy individuals and in a large variety of mental health and neuropsychiatric disorders [31].

Competing interests

No competing interest is declared.

Author contributions statement

M.M.M. conceived the experiment, analysed the data, and wrote the manuscript.

Acknowledgments

This work is supported in part by funds from the NIH (R01GM135420), DOD (TP230324), and the Brain Injury Research Center at UCLA. Data were provided by the Human Connectome Project, WU-Minn Consortium (Principal Investigators: David Van Essen and Kamil Ugurbil; 1U54MH091657) funded by the 16 NIH Institutes and Centers that support the NIH Blueprint for Neuroscience Research; and by the McDonnell Center for Systems Neuroscience at Washington University. The author would also like to acknowledge the UCLA Institute for Digital Research and Education (IDRE) for making temporarily available to investigators large space and computational resources for allowing processing and analysis of large datasets.

References

1. Keene Alex C., Duboue Erik R.. The origins and evolution of sleep *Journal of Experimental Biology.* 2018;221:jeb159533.
2. Walker Matthew P. The role of sleep in cognition and emotion *Annals of the New York Academy of Sciences.* 2009;1156:168–197.
3. Goldstein Andrea N, Walker Matthew P. The role of sleep in emotional brain function *Annual review of clinical psychology.* 2014;10:679–708.
4. Djonlagic Ina, Mariani Sara, Fitzpatrick Annette L, et al. Macro and micro sleep architecture and cognitive performance in older adults *Nature human behaviour.* 2021;5:123–145.
5. Yaffe Kristine, Falvey Cherie M, Hoang Tina. Connections between sleep and cognition in older adults *The Lancet Neurology.* 2014;13:1017–1028.
6. Galván Adriana. The need for sleep in the adolescent brain *Trends in cognitive sciences.* 2020;24:79–89.
7. Lim Julian, Dinges David F. A meta-analysis of the impact of short-term sleep deprivation on cognitive variables. *Psychological bulletin.* 2010;136:375.
8. Krause Adam J, Simon Eti Ben, Mander Bryce A, et al. The sleep-deprived human brain *Nature Reviews Neuroscience.* 2017;18:404–418.
9. Simon Eti Ben, Vallat Raphael, Barnes Christopher M, Walker Matthew P. Sleep loss and the socio-emotional brain *Trends in Cognitive Sciences.* 2020;24:435–450.
10. García Aída, Del Angel Jacqueline, Borrani Jorge, Ramirez Candelaria, Valdez Pablo. Sleep deprivation effects on basic cognitive processes: which components of attention, working memory, and executive functions are more susceptible to the lack of sleep? *Sleep Science.* 2021;14:107.
11. Tomaso Cara C, Johnson Anna B, Nelson Timothy D. The effect of sleep deprivation and restriction on mood, emotion, and emotion regulation: three meta-analyses in one *Sleep.* 2021;44:zsaa289.
12. Li Jiahui, Cao Yixuan, Ou Simei, Jiang Tianxiang, Wang Ling, Ma Ning. The effect of total sleep deprivation on working memory: evidence from diffusion model *Sleep.* 2024:zsae006.
13. Koyanagi Ai, Stickley Andrew. The Association between Sleep Problems and Psychotic Symptoms in the General Population: A Global Perspective *Sleep.* 2015;38:1875-1885.
14. Freeman Daniel, Sheaves Bryony, Waite Felicity, Harvey Allison G, Harrison Paul J. Sleep disturbance and psychiatric disorders *The Lancet Psychiatry.* 2020;7:628–637.
15. Cheng Wei, Rolls Edmund, Gong Weikang, et al. Sleep duration, brain structure, and psychiatric and cognitive problems in children *Molecular psychiatry.* 2021;26:3992–4003.
16. Sun Xiaohui, Liu Bin, Liu Sitong, et al. Sleep disturbance and psychiatric disorders: a bidirectional Mendelian randomisation study *Epidemiology and Psychiatric Sciences.* 2022;31:e26.
17. Emser W, Brenner M, Stober T, Schimrigk K. Changes in nocturnal sleep in Huntington's and Parkinson's disease *Journal of neurology.* 1988;235:177–179.
18. Morton A Jennifer, Wood Nigel I, Hastings Michael H, Hurelbrink Carrie, Barker Roger A, Maywood Elizabeth S. Disintegration of the sleep-wake cycle and circadian timing in Huntington's disease *Journal of Neuroscience.* 2005;25:157–163.
19. Zhang Ye, Ren Rong, Yang Linghui, et al. Sleep in Huntington's disease: a systematic review and meta-analysis of polysomongraphic findings *Sleep.* 2019;42:zsz154.
20. Stefani Ambra, Högl Birgit. Sleep in Parkinson's disease *Neuropsychopharmacology.* 2020;45:121–128.
21. Romanella SM, Roe D, Tatti E, et al. The sleep side of aging and Alzheimer's disease *Sleep medicine.* 2021;77:209–225.
22. Oh Jun Y., Walsh Christine M., Ranasinghe Kamalini, et al. Subcortical Neuronal Correlates of Sleep in Neurodegenerative Diseases *JAMA Neurology.* 2022;79:498-508.
23. Lima Santos João Paulo, Hayes Rebecca, Franzen Peter L, et al. The association between cortical gyrification and sleep in adolescents and young adults *Sleep.* 2024;47:zsad282.
24. Wei Ruoqi, Ganglberger Wolfgang, Sun Haoqi, et al. Linking brain structure, cognition, and sleep: insights from clinical data *Sleep.* 2024;47:zsad294.
25. Westwood Andrew J, Beiser Alexa, Jain Nikita, et al. Prolonged sleep duration as a marker of early neurodegeneration predicting incident dementia *Neurology.* 2017;88:1172–1179.
26. Fjell Anders M, Sørensen Øystein, Amlien Inge K, et al. Self-reported sleep relates to hippocampal atrophy across the adult lifespan: results from the Lifebrain consortium *Sleep.* 2020;43:zsz280.
27. Toschi Nicola, Passamonti Luca, Bellesi Michele. Sleep quality relates to emotional reactivity via intracortical myelination *Sleep.* 2021;44:zsaa146.
28. Schiel Julian E, Tamm Sandra, Holub Florian, et al. Associations between sleep health and grey matter volume in the UK Biobank cohort (n= 33 356) *Brain communications.* 2023;5:fcad200.
29. Stolicyn Aleks, Lyall Laura M, Lyall Donald M, et al. Comprehensive assessment of sleep duration, insomnia, and brain structure within the UK Biobank cohort *Sleep.* 2024;47:zsad274.
30. Spiegelhalder Kai, Riemann Dieter, Schiel Julian. Are sleep and brain structure associated in the UK Biobank? A letter to the editor regarding "Comprehensive assessment of sleep duration, insomnia and brain structure within the UK Biobank cohort." by Stolicyn et al. *Sleep.*

2023;47:zsad317.
31. Hasegawa Harutomo, Selway Richard, Gnoni Valentina, et al. The subcortical belly of sleep: New possibilities in neuromodulation of basal ganglia? *Sleep medicine reviews.* 2020;52:101317.
32. Van Essen David C, Smith Stephen M, Barch Deanna M, et al. The WU-Minn human connectome project: an overview *Neuroimage.* 2013;80:62–79.
33. Buysse Daniel J, Reynolds III Charles F, Monk Timothy H, Berman Susan R, Kupfer David J. The Pittsburgh Sleep Quality Index: a new instrument for psychiatric practice and research *Psychiatry research.* 1989;28:193–213.
34. Ashburner John, Friston Karl J. Voxel-based morphometry—the methods *Neuroimage.* 2000;11:805–821.
35. Good Catriona D, Johnsrude Ingrid S, Ashburner John, Henson Richard NA, Friston Karl J, Frackowiak Richard SJ. A voxel-based morphometric study of ageing in 465 normal adult human brains *Neuroimage.* 2001;14:21–36.
36. Patenaude Brian, Smith Stephen M, Kennedy David N, Jenkinson Mark. A Bayesian model of shape and appearance for subcortical brain segmentation *Neuroimage.* 2011;56:907–922.
37. Pearson Karl. LIII. On lines and planes of closest fit to systems of points in space *The London, Edinburgh, and Dublin philosophical magazine and journal of science.* 1901;2:559–572.
38. JASP Team . JASP (Version 0.18.3)[Computer software] 2024.
39. Lutkenhoff Evan S, Wright Matthew J, Shrestha Vikesh, et al. The subcortical basis of outcome and cognitive impairment in TBI: A longitudinal cohort study *Neurology.* 2020;95:e2398–e2408.
40. Smith Stephen M, Jenkinson Mark, Woolrich Mark W, et al. Advances in functional and structural MR image analysis and implementation as FSL *Neuroimage.* 2004;23:S208–S219.
41. Zhang Yongyue, Brady Michael, Smith Stephen. Segmentation of brain MR images through a hidden Markov random field model and the expectation-maximization algorithm *IEEE transactions on medical imaging.* 2001;20:45–57.
42. Jenkinson Mark, Smith Stephen. A global optimisation method for robust affine registration of brain images *Medical image analysis.* 2001;5:143–156.
43. Jenkinson Mark, Bannister Peter, Brady Michael, Smith Stephen. Improved optimization for the robust and accurate linear registration and motion correction of brain images *Neuroimage.* 2002;17:825–841.
44. Douaud Gwenaëlle, Smith Stephen, Jenkinson Mark, et al. Anatomically related grey and white matter abnormalities in adolescent-onset schizophrenia *Brain.* 2007;130:2375–2386.
45. Smith Stephen M, Zhang Yongyue, Jenkinson Mark, et al. Accurate, robust, and automated longitudinal and cross-sectional brain change analysis *Neuroimage.* 2002;17:479–489.
46. Lutkenhoff Evan S, Chiang Jeffrey, Tshibanda Luaba, et al. Thalamic and extrathalamic mechanisms of consciousness after severe brain injury *Annals of neurology.* 2015;78:68–76.
47. Winkler Anderson M, Ridgway Gerard R, Webster Matthew A, Smith Stephen M, Nichols Thomas E. Permutation inference for the general linear model *Neuroimage.* 2014;92:381–397.
48. Nichols Thomas E, Holmes Andrew P. Nonparametric permutation tests for functional neuroimaging: a primer with examples *Human brain mapping.* 2002;15:1–25.
49. Smith Stephen M, Nichols Thomas E. Threshold-free cluster enhancement: addressing problems of smoothing, threshold dependence and localisation in cluster inference *Neuroimage.* 2009;44:83–98.
50. Salimi-Khorshidi Gholamreza, Smith Stephen M, Nichols Thomas E. Adjusting the effect of nonstationarity in cluster-based and TFCE inference *Neuroimage.* 2011;54:2006–2019.
51. Zhou Xinqi, Wu Renjing, Zeng Yixu, et al. Choice of voxel-based morphometry processing pipeline drives variability in the location of neuroanatomical brain markers *Communications Biology.* 2022;5:913.
52. Glasser Matthew F, Sotiropoulos Stamatios N, Wilson J Anthony, et al. The minimal preprocessing pipelines for the Human Connectome Project *Neuroimage.* 2013;80:105–124.
53. Dale Anders M, Fischl Bruce, Sereno Martin I. Cortical surface-based analysis: I. Segmentation and surface reconstruction *Neuroimage.* 1999;9:179–194.
54. Fischl Bruce, Sereno Martin I, Dale Anders M. Cortical surface-based analysis: II: inflation, flattening, and a surface-based coordinate system *Neuroimage.* 1999;9:195–207.
55. Shapiro Samuel Sanford, Wilk Martin B. An analysis of variance test for normality (complete samples) *Biometrika.* 1965;52:591–611.
56. Benjamini Yoav, Yekutieli Daniel. False discovery rate–adjusted multiple confidence intervals for selected parameters *Journal of the American Statistical Association.* 2005;100:71–81.
57. Gadea-Ciria M, Stabler H, Lloyd KG, Bartholini G. Acetylcholine release within the cat striatum during the sleep–wakefulness cycle *Nature.* 1973;243:518–519.
58. Corsi-Cabrera M, Grinberg-Zylberbaum J, Arditti LS. Caudate nucleus lesion selectively increases paradoxical sleep episodes in the rat *Physiology & behavior.* 1975;14:7–11.
59. Lazarus Michael, Huang Zhi-Li, Lu Jun, Urade Yoshihiro, Chen Jiang-Fan. How do the basal ganglia regulate sleep–wake behavior? *Trends in neurosciences.* 2012;35:723–732.
60. Lazarus Michael, Chen Jiang-Fan, Urade Yoshihiro, Huang Zhi-Li. Role of the basal ganglia in the control of sleep and wakefulness *Current opinion in neurobiology.* 2013;23:780–785.
61. Saper Clifford B, Fuller Patrick M, Pedersen Nigel P, Lu Jun, Scammell Thomas E. Sleep state switching *Neuron.* 2010;68:1023–1042.
62. Whyte Christopher J., Redinbaugh Michelle J., Shine James M., Saalmann Yuri B.. Thalamic contributions to the state and contents of consciousness *Neuron.* 2024;112:1611-1625.
63. Li Min, Wang Ruonan, Zhao Meng, et al. Abnormalities of thalamus volume and resting state functional connectivity in primary insomnia patients *Brain Imaging and Behavior.* 2019;13:1193–1201.

64. Zou Guangyuan, Li Yuezhen, Liu Jiayi, et al. Altered thalamic connectivity in insomnia disorder during wakefulness and sleep *Human brain mapping.* 2021;42:259–270.
65. Ma Xueying, Zhang Yan, Ma Shaohui, et al. Association between abnormal thalamic metabolites and sleep disturbance in patients with end-stage renal disease *Metabolic brain disease.* 2018;33:1641–1648.
66. Wang Jian, Huang Cigui, Luo Guowei, et al. Reduced sleep quality defines a subtype of obsessive-compulsive disorder with lower Glx levels in the resting thalamus and worse response inhibition *Journal of Psychiatric Research.* 2024;173:14–24.
67. Liu Chunlei, Kong Xiang-zhen, Liu Xueyong, Zhou Renlai, Wu Bin. Long-term total sleep deprivation reduces thalamic gray matter volume in healthy men *Neuroreport.* 2014;25:320–323.
68. Wu Wei, Cui Linyang, Fu Ying, et al. Sleep and cognitive abnormalities in acute minor thalamic infarction *Neuroscience bulletin.* 2016;32:341–348.
69. Li Q, Zhao X, Gong DH, Geng YM, Zhang HL, Bi PX. Sleep disorders of acute thalamic stroke and its influence on plasma IL-17. *Journal of Biological Regulators and Homeostatic Agents.* 2017;31:745–751.
70. Liu Chun-Hong, Liu Cun-Zhi, Zhang Jihui, et al. Reduced spontaneous neuronal activity in the insular cortex and thalamus in healthy adults with insomnia symptoms *Brain research.* 2016;1648:317–324.
71. Wilson SA Kinnier. Modern problems in neurology *British Medical Journal.* 1928;2:914.
72. Gerfen Charles R, Bolam J Paul. The neuroanatomical organization of the basal ganglia in *Handbook of behavioral neuroscience*;24:3–32Elsevier 2016.
73. Zheng Zhong S, Monti Martin M. Cortical and thalamic connections of the human globus pallidus: Implications for disorders of consciousness *Frontiers in Neuroanatomy.* 2022;16:960439.
74. Menza Matthew, Dobkin Roseanne DeFronzo, Marin Humberto, Bienfait Karina. Sleep disturbances in Parkinson's disease *Movement Disorders.* 2010;25:S117–S122.
75. Lima Marcelo MS. Sleep disturbances in Parkinson's disease: the contribution of dopamine in REM sleep regulation *Sleep medicine reviews.* 2013;17:367–375.
76. Lee Bi-Fang, Chiu Nan-Tsing, Yang Yen Kuang, Chu Ching Lin. The relation between striatal dopamine D2/D3 receptor availability and sleep quality in healthy adults *Nuclear Medicine Communications.* 2007;28:401–406.
77. Mena-Segovia Juan, Cintra León, Prospéro-Garcıa Oscar, Giordano Magda. Changes in sleep–waking cycle after striatal excitotoxic lesions *Behavioural brain research.* 2002;136:475–481.
78. Qiu Mei-Hong, Vetrivelan Ramalingam, Fuller Patrick M, Lu Jun. Basal ganglia control of sleep–wake behavior and cortical activation *European Journal of Neuroscience.* 2010;31:499–507.
79. Monti Jaime M, Monti Daniel. The involvement of dopamine in the modulation of sleep and waking *Sleep medicine reviews.* 2007;11:113–133.
80. Oishi Yo, Lazarus Michael. The control of sleep and wakefulness by mesolimbic dopamine systems *Neuroscience research.* 2017;118:66–73.
81. Albin Roger L, Young Anne B, Penney John B. The functional anatomy of basal ganglia disorders *Trends in neurosciences.* 1989;12:366–375.
82. Alexander Garrett E, Crutcher Michael D. Functional architecture of basal ganglia circuits: neural substrates of parallel processing *Trends in neurosciences.* 1990;13:266–271.
83. Nambu Atsushi, Tokuno Hironobu, Takada Masahiko. Functional significance of the cortico–subthalamo–pallidal 'hyperdirect'pathway *Neuroscience research.* 2002;43:111–117.
84. Qiu Mei-Hong, Zhong Zhi-Gang, Chen Michael C, Lu Jun. Nigrostriatal and mesolimbic control of sleep–wake behavior in rat *Brain Structure and Function.* 2019;224:2525–2535.
85. Qiu Mei-Hong, Yao Qiao-Ling, Vetrivelan Ramalingam, Chen Michael C, Lu Jun. Nigrostriatal dopamine acting on globus pallidus regulates sleep *Cerebral cortex.* 2016;26:1430–1439.
86. Qiu MH, Chen Michael C, Wu Jianping, Nelson Dwight, Lu Jun. Deep brain stimulation in the globus pallidus externa promotes sleep *Neuroscience.* 2016;322:115–120.
87. Crone Julia Sophia, Lutkenhoff Evan Scott, Bio Branden Joseph, Laureys Steven, Monti Martin Max. Testing proposed neuronal models of effective connectivity within the cortico-basal ganglia-thalamo-cortical loop during loss of consciousness *Cerebral Cortex.* 2017;27:2727–2738.
88. Castillo Pablo R, Middlebrooks Erik H, Grewal Sanjeet S, et al. Globus pallidus externus deep brain stimulation treats insomnia in a patient with Parkinson disease in *Mayo Clinic Proceedings*;95:419–422Elsevier 2020.
89. Poulin Stéphane P, Dautoff Rebecca, Morris John C, et al. Amygdala atrophy is prominent in early Alzheimer's disease and relates to symptom severity *Psychiatry Research: Neuroimaging.* 2011;194:7–13.
90. Zhang Rui, Tomasi Dardo, Manza Peter, et al. Sleep disturbances are associated with cortical and subcortical atrophy in alcohol use disorder *Translational psychiatry.* 2021;11:428.
91. Yu Honghui, Chen Liting, Li Haijun, et al. Abnormal resting-state functional connectivity of amygdala subregions in patients with obstructive sleep apnea *Neuropsychiatric disease and treatment.* 2019:977–987.
92. Burdová K, Filip P, Šonka K, et al. Hippocampal and amygdala atrophy rates correlate with the severity of sleep apnoea in Parkinson's disease *Parkinsonism & Related Disorders.* 2023;113.
93. Gong Liang, Liao Tianzhi, Liu Duan, et al. Amygdala changes in chronic insomnia and their association with sleep and anxiety symptoms: insight from shape analysis *Neural plasticity.* 2019;2019.
94. Chao Linda L, Mohlenhoff Brian S, Weiner Michael W, Neylan Thomas C. Associations between subjective sleep quality and brain volume in Gulf War veterans *Sleep.* 2014;37:445–452.
95. Duffau Hugues. A two-level model of interindividual anatomo-functional variability of the brain and its implications for neurosurgery *Cortex.* 2017;86:303–313.
96. Kroeger Daniel, Vetrivelan Ramalingam. To sleep or not to sleep–Effects on memory in normal aging and disease *Aging Brain.* 2023;3:100068.
97. Vetrivelan Ramalingam, Bandaru Sathyajit Sai. Neural Control of REM Sleep and Motor Atonia: Current Perspectives *Current Neurology and Neuroscience Reports.* 2023;23:907–923.

98. Reddy Oliver Cameron, Werf Ysbrand D. The sleeping brain: harnessing the power of the glymphatic system through lifestyle choices *Brain sciences.* 2020;10:868.
99. Dai Xi-Jian, Peng De-Chang, Gong Hong-Han, et al. Altered intrinsic regional brain spontaneous activity and subjective sleep quality in patients with chronic primary insomnia: a resting-state fMRI study *Neuropsychiatric disease and treatment.* 2014:2163–2175.
100. Komarov Oleksii, Ko Li-Wei, Jung Tzyy-Ping. Associations among emotional state, sleep quality, and resting-state EEG spectra: a longitudinal study in graduate students *IEEE Transactions on Neural Systems and Rehabilitation Engineering.* 2020;28:795–804.
101. Venkataraman Arun, Zhuang Yuchuan, Marsella Jennifer, et al. Functional MRI correlates of sleep quality in HIV *Nature and science of sleep.* 2021:291–301.
102. He Dongmei, Ren Dongmei, Guo Zhiwei, Jiang Binghu. Insomnia disorder diagnosed by resting-state fMRI-based SVM classifier *Sleep Medicine.* 2022;95:126–129.
103. Picchioni Dante, Pixa Morgan L, Fukunaga Masaki, et al. Decreased connectivity between the thalamus and the neocortex during human nonrapid eye movement sleep *Sleep.* 2014;37:387–397.
104. Zhou Zhongxing, Cai Biao, Zhang Gemeng, Zhang Aiying, Calhoun Vince D, Wang Yu-Ping. Prediction and classification of sleep quality based on phase synchronization related whole-brain dynamic connectivity using resting state fMRI *NeuroImage.* 2020;221:117190.

Supplementary Online Materials

Table SOM1: Comparison of HCP volumetric data for 'good sleepers' versus 'bad sleepers.' (Abbreviations: 'W' is the statistic value for a two-sample Mann-Whitney test; 'p (unc)' is the uncorrected p-value; 'p (FDR)' is the FDR-corrected p-value; 'RBC' is the rank biserial correlation statistic, as a measure of effect size.)

Measure	W	p (unc)	p (FDR)	RBC
Global measurements				
FS_IntraCranial_Vol	124,866.0	0.062	0.274	-0.069
FS_BrainSeg_Vol	123,531.0	0.033	0.211	-0.079
FS_BrainSeg_Vol_No_Vent	123,128.5	0.027	0.206	-0.082
FS_BrainSeg_Vol_No_Vent_Surf	123,148.0	0.027	0.206	-0.082
FS_LCort_GM_Vol	121,509.5	0.011	0.144	-0.094
FS_RCort_GM_Vol	121,625.5	0.012	0.144	-0.093
FS_TotCort_GM_Vol	121,625.0	0.012	0.144	-0.093
FS_SubCort_GM_Vol	127,105.5	0.157	0.370	-0.053
FS_Total_GM_Vol	121,207.5	0.009	0.144	-0.097
FS_SupraTentorial_Vol	123,960.0	0.041	0.221	-0.076
FS_L_WM_Vol	125,005.5	0.066	0.274	-0.068
FS_R_WM_Vol	125,156.5	0.071	0.281	-0.067
FS_Tot_WM_Vol	125,085.0	0.069	0.280	-0.068
FS_Mask_Vol	123,686.5	0.036	0.211	-0.078
FS_BrainSegVol_eTIV_Ratio	135,420.5	0.802	0.890	0.009
FS_MaskVol_eTIV_Ratio	136,947.0	0.577	0.750	0.021
FS_LH_Defect_Holes	138,301.5	0.407	0.618	0.031
FS_RH_Defect_Holes	142,803.5	0.083	0.306	0.064
FS_Total_Defect_Holes	141,508.0	0.141	0.352	0.055
Volume measurements				
FS_L_LatVent_Vol	132,341.5	0.715	0.855	-0.014
FS_L_InfLatVent_Vol	139,308.5	0.303	0.535	0.038
FS_L_Cerebellum_WM_Vol	131,087.0	0.537	0.723	-0.023
FS_L_Cerebellum_Cort_Vol	122,764.0	0.022	0.190	-0.085
FS_L_ThalamusProper_Vol	131,224.5	0.556	0.741	-0.022
FS_L_Caudate_Vol	126,520.0	0.125	0.336	-0.057
FS_L_Putamen_Vol	125,656.0	0.088	0.313	-0.063
FS_L_Pallidum_Vol	133,291.5	0.861	0.926	-0.007
FS_3rdVent_Vol	131,494.5	0.592	0.755	-0.020
FS_4thVent_Vol	126,041.5	0.103	0.313	-0.061
FS_BrainStem_Vol	131,858.0	0.644	0.809	-0.017
FS_L_Hippo_Vol	125,997.0	0.102	0.313	-0.061
FS_L_Amygdala_Vol	128,120.0	0.226	0.454	-0.045
FS_CSF_Vol	131,807.5	0.636	0.806	-0.018
FS_L_AccumbensArea_Vol	127,153.5	0.160	0.370	-0.052
FS_L_VentDC_Vol	129,789.0	0.380	0.595	-0.033
FS_L_Vessel_Vol	127,965.0	0.214	0.439	-0.046
FS_L_ChoroidPlexus_Vol	140,640.5	0.194	0.413	0.048
FS_R_LatVent_Vol	133,406.5	0.879	0.935	-0.006
FS_R_InfLatVent_Vol	134,051.0	0.982	1.000	-89.71
FS_R_Cerebellum_WM_Vol	129,428.0	0.342	0.579	-0.035
FS_R_Cerebellum_Cort_Vol	122,961.5	0.025	0.206	-0.084
FS_R_ThalamusProper_Vol	129,445.0	0.344	0.579	-0.035
FS_R_Caudate_Vol	127,757.0	0.199	0.413	-0.048
FS_R_Putamen_Vol	130,254.0	0.433	0.643	-0.029
FS_R_Pallidum_Vol	132,734.5	0.774	0.879	-0.011
FS_R_Hippo_Vol	124,059.5	0.043	0.225	-0.075
FS_R_Amygdala_Vol	124,901.0	0.063	0.274	-0.069
FS_R_AccumbensArea_Vol	123,934.0	0.040	0.221	-0.076
FS_R_VentDC_Vol	130,550.5	0.469	0.667	-0.027
FS_R_Vessel_Vol	135,146.5	0.844	0.918	0.007
FS_R_ChoroidPlexus_Vol	139,200.0	0.313	0.542	0.038
FS_5thVent_Vol	143,599.0	0.049	0.238	0.070
FS_WM_Hypointens_Vol	133,779.0	0.938	0.982	-0.003
FS_L_WM_Hypointens_Vol	.	.	.	.
FS_R_WM_Hypointens_Vol	.	.	.	.
FS_L_Non-WM_Hypointens_Vol	.	.	.	.

FS_R_Non-WM_Hypointens_Vol	.	.	.	.
FS_OpticChiasm_Vol	138,370.0	0.399	0.618	0.031
FS_CC_Posterior_Vol	126,883.5	0.144	0.352	-0.054
FS_CC_MidPosterior_Vol	125,893.0	0.097	0.313	-0.062
FS_CC_Central_Vol	129,656.0	0.366	0.587	-0.034
FS_CC_MidAnterior_Vol	126,003.0	0.102	0.313	-0.061
FS_CC_Anterior_Vol	130,404.0	0.451	0.663	-0.028
Thickness measurements				
FS_L_Bankssts_Thck	133,237.0	0.852	0.921	-0.007
FS_L_Caudalanteriorcingulate_Thck	127,395.5	0.175	0.394	-0.050
FS_L_Caudalmiddlefrontal_Thck	137,429.0	0.513	0.709	0.024
FS_L_Cuneus_Thck	126,083.0	0.105	0.313	-0.060
FS_L_Entorhinal_Thck	118,507.0	0.002	0.114	-0.117
FS_L_Fusiform_Thck	131,092.5	0.538	0.723	-0.023
FS_L_Inferiorparietal_Thck	132,952.0	0.808	0.893	-0.009
FS_L_Inferiortemporal_Thck	131,069.0	0.535	0.723	-0.023
FS_L_Isthmuscingulate_Thck	131,330.0	0.570	0.746	-0.021
FS_L_Lateraloccipital_Thck	128,683.0	0.272	0.506	-0.041
FS_L_Lateralorbitofrontal_Thck	132,080.0	0.676	0.825	-0.016
FS_L_Lingual_Thck	129,730.0	0.374	0.591	-0.033
FS_L_Medialorbitofrontal_Thck	137,501.5	0.504	0.701	0.025
FS_L_Middletemporal_Thck	133,517.0	0.897	0.948	-0.005
FS_L_Parahippocampal_Thck	141,622.5	0.135	0.349	0.056
FS_L_Paracentral_Thck	130,737.0	0.492	0.694	-0.026
FS_L_Parsopercularis_Thck	135,437.5	0.799	0.890	0.009
FS_L_Parsorbitalis_Thck	138,672.0	0.366	0.587	0.034
FS_L_Parstriangularis_Thck	135,175.0	0.840	0.918	0.008
FS_L_Pericalcarine_Thck	127,725.5	0.197	0.413	-0.048
FS_L_Postcentral_Thck	131,281.5	0.563	0.742	-0.021
FS_L_Posteriorcingulate_Thck	128,340.5	0.243	0.484	-0.043
FS_L_Precentral_Thck	135,995.0	0.714	0.855	0.014
FS_L_Precuneus_Thck	126,681.5	0.134	0.349	-0.056
FS_L_Rostralanteriorcingulate_Thck	129,037.0	0.304	0.535	-0.038
FS_L_Rostralmiddlefrontal_Thck	134,789.5	0.901	0.949	0.005
FS_L_Superiorfrontal_Thck	135,520.5	0.786	0.884	0.010
FS_L_Superiorparietal_Thck	136,876.0	0.587	0.754	0.020
FS_L_Superiortemporal_Thck	135,906.5	0.727	0.856	0.013
FS_L_Supramarginal_Thck	135,733.0	0.754	0.866	0.012
FS_L_Frontalpole_Thck	132,533.5	0.744	0.866	-0.012
FS_L_Temporalpole_Thck	128,505.0	0.257	0.493	-0.042
FS_L_Transversetemporal_Thck	126,679.5	0.133	0.349	-0.056
FS_L_Insula_Thck	133,873.5	0.953	0.993	-0.002
FS_R_Bankssts_Thck	126,041.0	0.103	0.313	-0.061
FS_R_Caudalanteriorcingulate_Thck	138,314.0	0.406	0.618	0.031
FS_R_Caudalmiddlefrontal_Thck	130,806.0	0.501	0.701	-0.025
FS_R_Cuneus_Thck	129,025.0	0.303	0.535	-0.038
FS_R_Entorhinal_Thck	116,172.5	<0.001	<0.001	-0.134
FS_R_Fusiform_Thck	126,940.0	0.148	0.352	-0.054
FS_R_Inferiorparietal_Thck	133,939.0	0.964	0.999	-0.002
FS_R_Inferiortemporal_Thck	127,683.5	0.194	0.413	-0.048
FS_R_Isthmuscingulate_Thck	136,180.0	0.687	0.832	0.015
FS_R_Lateraloccipital_Thck	130,024.5	0.406	0.618	-0.031
FS_R_Lateralorbitofrontal_Thck	128,854.5	0.287	0.529	-0.040
FS_R_Lingual_Thck	134,068.5	0.984	1.000	-76.67
FS_R_Medialorbitofrontal_Thck	139,885.0	0.252	0.492	0.043
FS_R_Middletemporal_Thck	129,628.5	0.363	0.587	-0.034
FS_R_Parahippocampal_Thck	137,801.5	0.466	0.667	0.027
FS_R_Paracentral_Thck	125,176.0	0.072	0.281	-0.067
FS_R_Parsopercularis_Thck	137,865.5	0.458	0.663	0.028
FS_R_Parsorbitalis_Thck	132,598.5	0.753	0.866	-0.012
FS_R_Parstriangularis_Thck	135,969.0	0.718	0.855	0.013
FS_R_Pericalcarine_Thck	138,868.5	0.346	0.579	0.035
FS_R_Postcentral_Thck	134,981.0	0.870	0.931	0.006
FS_R_Posteriorcingulate_Thck	127,480.5	0.180	0.398	-0.050

FS_R_Precentral_Thck	136,250.5	0.676	0.825	0.016
FS_R_Precuneus_Thck	129,004.5	0.301	0.535	-0.038
FS_R_Rostralanteriorcingulate_Thck	144,988.0	0.030	0.206	0.081
FS_R_Rostralmiddlefrontal_Thck	137,064.0	0.561	0.742	0.022
FS_R_Superiorfrontal_Thck	132,999.5	0.815	0.896	-0.009
FS_R_Superiorparietal_Thck	136,259.0	0.675	0.825	0.016
FS_R_Superiortemporal_Thck	135,576.0	0.778	0.879	0.011
FS_R_Supramarginal_Thck	135,734.5	0.753	0.866	0.012
FS_R_Frontalpole_Thck	138,767.5	0.356	0.587	0.034
FS_R_Temporalpole_Thck	116,450.5	<0.001	<0.001	-0.132
FS_R_Transversetemporal_Thck	129,339.5	0.333	0.571	-0.036
FS_R_Insula_Thck	131,919.0	0.652	0.811	-0.017
Area measurements				
FS_L_Bankssts_Area	129,087.5	0.309	0.539	-0.038
FS_L_Caudalanteriorcingulate_Area	123,190.0	0.028	0.206	-0.082
FS_L_Caudalmiddlefrontal_Area	128,617.5	0.266	0.499	-0.041
FS_L_Cuneus_Area	126,126.5	0.107	0.313	-0.060
FS_L_Entorhinal_Area	124,959.5	0.065	0.274	-0.069
FS_L_Fusiform_Area	123,662.0	0.035	0.211	-0.078
FS_L_Inferiorparietal_Area	126,068.0	0.105	0.313	-0.060
FS_L_Inferiortemporal_Area	122,201.5	0.016	0.168	-0.089
FS_L_Isthmuscingulate_Area	130,172.5	0.423	0.633	-0.030
FS_L_Lateraloccipital_Area	128,006.0	0.217	0.441	-0.046
FS_L_Lateralorbitofrontal_Area	119,886.0	0.004	0.114	-0.106
FS_L_Lingual_Area	127,615.5	0.189	0.413	-0.049
FS_L_Medialorbitofrontal_Area	124,544.0	0.054	0.256	-0.072
FS_L_Middletemporal_Area	123,990.0	0.041	0.221	-0.076
FS_L_Parahippocampal_Area	125,426.5	0.080	0.306	-0.065
FS_L_Paracentral_Area	125,920.5	0.098	0.313	-0.061
FS_L_Parsopercularis_Area	121,715.0	0.013	0.144	-0.093
FS_L_Parsorbitalis_Area	120,630.0	0.007	0.139	-0.101
FS_L_Parstriangularis_Area	124,956.0	0.065	0.274	-0.069
FS_L_Pericalcarine_Area	126,397.0	0.119	0.329	-0.058
FS_L_Postcentral_Area	130,478.5	0.460	0.663	-0.027
FS_L_Posteriorcingulate_Area	131,871.5	0.646	0.809	-0.017
FS_L_Precentral_Area	124,223.0	0.046	0.229	-0.074
FS_L_Precuneus_Area	128,983.0	0.299	0.535	-0.039
FS_L_Rostralanteriorcingulate_Area	124,182.0	0.045	0.229	-0.074
FS_L_Rostralmiddlefrontal_Area	126,231.0	0.112	0.318	-0.059
FS_L_Superiorfrontal_Area	121,132.5	0.009	0.144	-0.097
FS_L_Superiorparietal_Area	121,779.0	0.013	0.144	-0.092
FS_L_Superiortemporal_Area	126,869.0	0.144	0.352	-0.054
FS_L_Supramarginal_Area	123,251.5	0.029	0.206	-0.081
FS_L_Frontalpole_Area	126,924.0	0.147	0.352	-0.054
FS_L_Temporalpole_Area	130,161.0	0.422	0.633	-0.030
FS_L_Transversetemporal_Area	126,447.0	0.122	0.333	-0.058
FS_L_Insula_Area	128,434.0	0.251	0.492	-0.043
FS_R_Bankssts_Area	126,366.5	0.118	0.329	-0.058
FS_R_Caudalanteriorcingulate_Area	127,422.0	0.176	0.394	-0.050
FS_R_Caudalmiddlefrontal_Area	129,584.0	0.358	0.587	-0.034
FS_R_Cuneus_Area	122,425.0	0.019	0.180	-0.088
FS_R_Entorhinal_Area	132,706.5	0.770	0.879	-0.011
FS_R_Fusiform_Area	129,696.0	0.370	0.589	-0.033
FS_R_Inferiorparietal_Area	127,199.5	0.163	0.373	-0.052
FS_R_Inferiortemporal_Area	121,251.0	0.010	0.144	-0.096
FS_R_Isthmuscingulate_Area	130,998.5	0.526	0.721	-0.024
FS_R_Lateraloccipital_Area	125,767.5	0.092	0.313	-0.063
FS_R_Lateralorbitofrontal_Area	119,606.5	0.004	0.114	-0.109
FS_R_Lingual_Area	126,011.0	0.102	0.313	-0.061
FS_R_Medialorbitofrontal_Area	120,810.5	0.007	0.139	-0.100
FS_R_Middletemporal_Area	120,611.0	0.007	0.139	-0.101
FS_R_Parahippocampal_Area	124,955.0	0.065	0.274	-0.069
FS_R_Paracentral_Area	131,451.0	0.586	0.754	-0.020
FS_R_Parsopercularis_Area	122,586.5	0.020	0.181	-0.086

FS_R_Parsorbitalis_Area	123,720.0	0.036	0.211	-0.078
FS_R_Parstriangularis_Area	127,728.5	0.197	0.413	-0.048
FS_R_Pericalcarine_Area	126,174.5	0.109	0.314	-0.060
FS_R_Postcentral_Area	130,430.0	0.454	0.663	-0.028
FS_R_Posteriorcingulate_Area	127,150.5	0.160	0.370	-0.052
FS_R_Precentral_Area	125,505.5	0.083	0.306	-0.065
FS_R_Precuneus_Area	128,552.5	0.261	0.493	-0.042
FS_R_Rostralanteriorcingulate_Area	133,984.5	0.971	1.000	-0.001
FS_R_Rostralmiddlefrontal_Area	123,631.0	0.035	0.211	-0.079
FS_R_Superiorfrontal_Area	119,260.0	0.003	0.114	-0.111
FS_R_Superiorparietal_Area	122,237.5	0.017	0.169	-0.089
FS_R_Superiortemporal_Area	125,674.0	0.089	0.313	-0.063
FS_R_Supramarginal_Area	119,919.0	0.004	0.114	-0.106
FS_R_Frontalpole_Area	128,546.0	0.260	0.493	-0.042
FS_R_Temporalpole_Area	132,393.5	0.722	0.855	-0.013
FS_R_Transversetemporal_Area	126,094.0	0.106	0.313	-0.060
FS_R_Insula_Area	126,919.0	0.146	0.352	-0.054

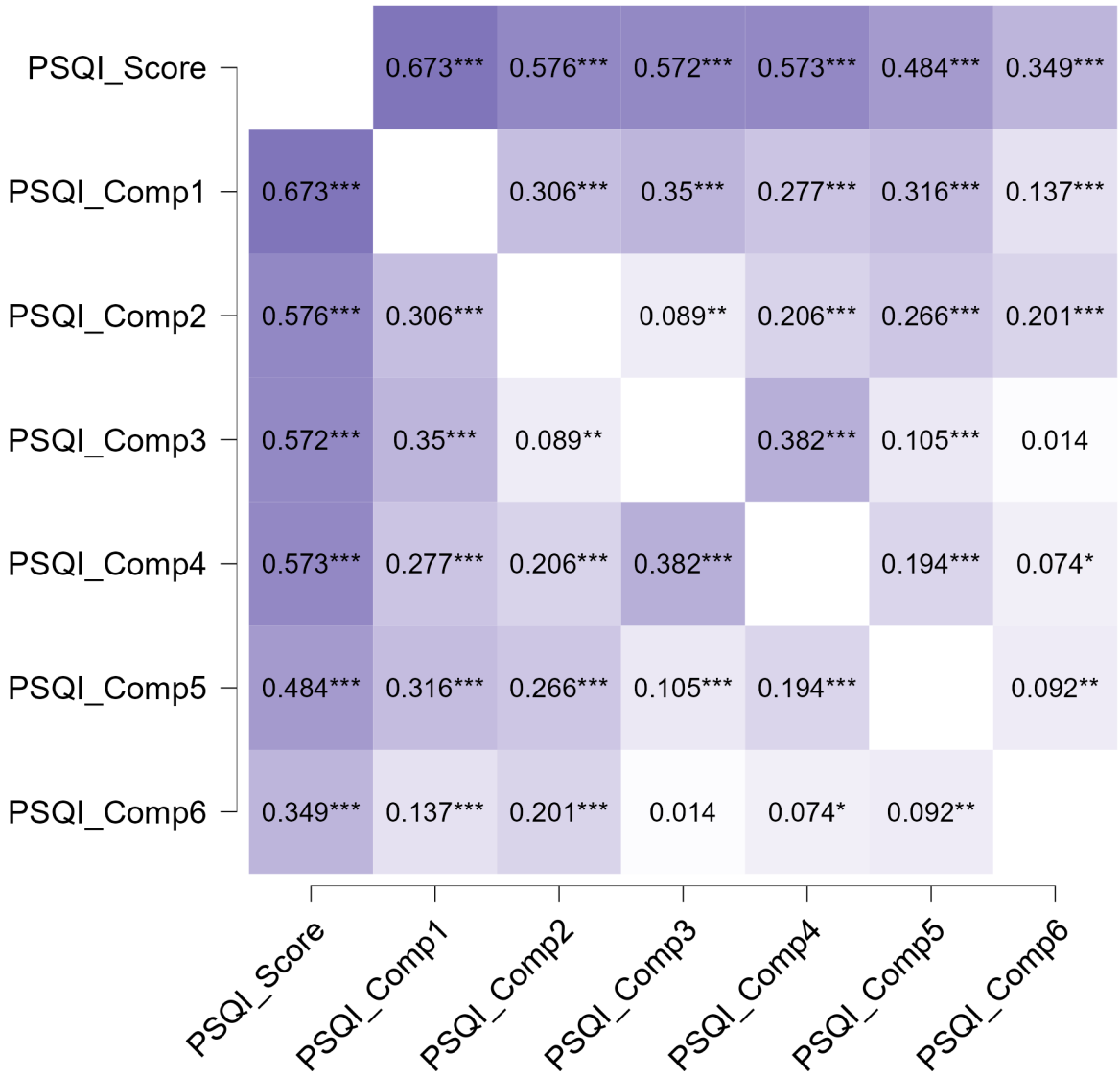

Fig. SOM1. Pairwise correlation coefficients (Spearman's ρ) between PSQI components ('*' indicates $p < 0.05$, '**' $p < 0.01$, '***' $p < 0.001$).

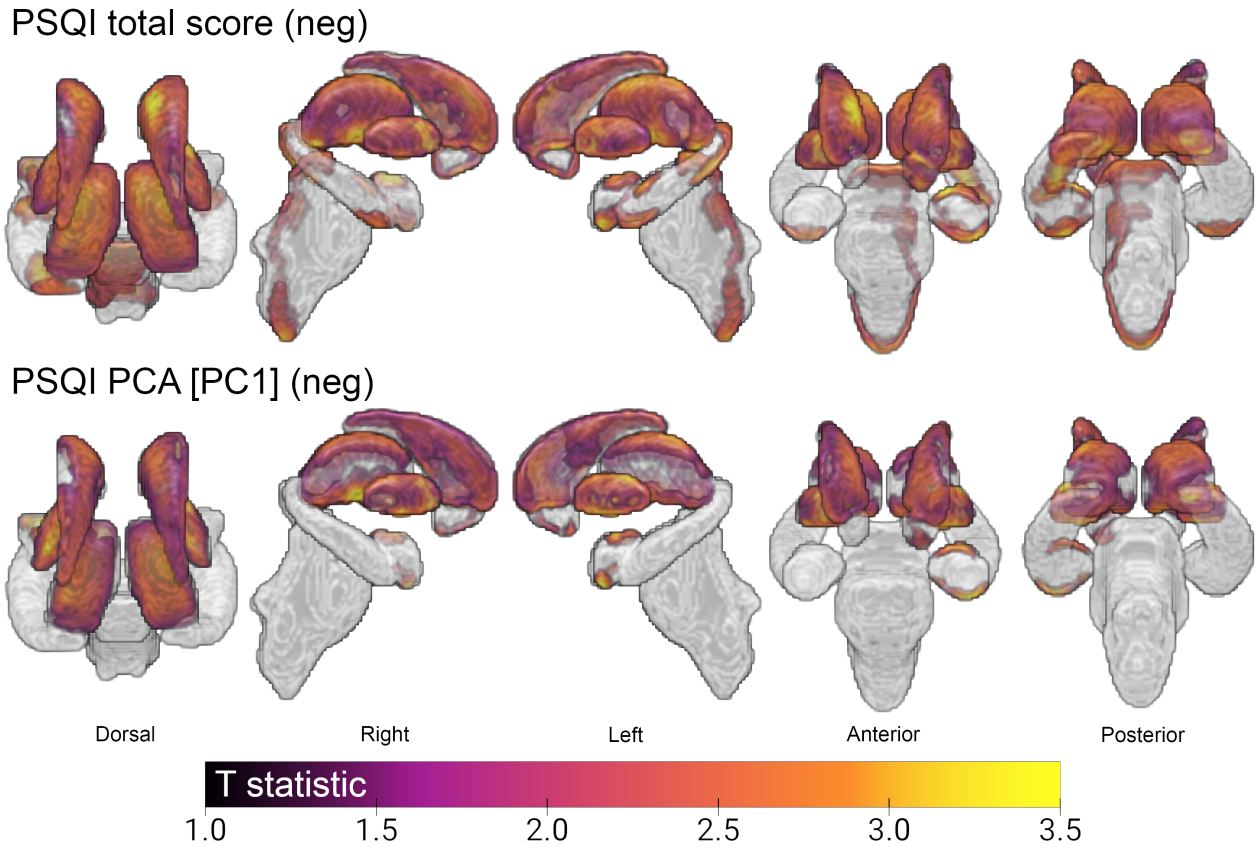

Fig. SOM2. Subcortical results for the PSQI and PSQI PC contrasts shown without the putamen so to reveal the lateral portion of the globus pallidus, caudate and thalamus. (All conventions and abbreviation are the same as in Fig. 3.)